Journal of Salutogenic Architecture

Original Scientific Paper

Journal of Salutogenic Architecture

2026, Volume 5, Issue 1, pages 01–21; https://doi.org/10.38027/jsalutogenic_vol5no1_1

Sustainable Design of Free-Form Architectural Shells Using Machine Learning and Parametric Optimization: A Case Study of the Rhike Park Music Theatre

Fatma Alemşah Kumtaş
Department of Informatics, Architectural Design Computing, Istanbul Technical University, Türkiye
kumtas24@itu.edu.tr
https://orcid.org/0009-0002-1099-9279

Abstract
Free-form architectural envelopes are visually striking but notoriously difficult and costly to build. This study explores how computational tools can make such designs more sustainable and constructible, using the Rhike Park Music Theatre in Tbilisi, Georgia, as a case study. The building's double-curved surfaces were reconstructed in Rhino/Grasshopper, and its façade was rationalized into a triangulated panel system. An evolutionary algorithm (Galapagos) first identified optimal panel configurations by balancing material use against fabrication simplicity. A neural network emulator, trained on 500 parametric simulations, was used to optimize the panelization process. The final design achieved an approximately 40% reduction in surface area, 55.6% fewer unique panel types, and retained 95% of the original interior volume. The proposed workflow demonstrates how ANN-based surrogate modelling can accelerate free-form façade optimization while maintaining geometric performance and manufacturability, contributing a computational framework for efficient design-space exploration.

Keywords*:* Parametric Design, Computational Optimization, Neural Network Emulator, Façade Panelization, Form-Finding.

Article History:
Received: 14 June 2026
Revised: 27 August 2026
Accepted: 2 September 2026
Available online: 3 September 2026

1. Introduction

1.1 Background and Context

Recent advancements in digital design technologies have significantly transformed architectural practice and enabled the widespread adoption of complex free-form façade systems. These developments now allow digitally produced free-form façade cladding to be designed and implemented at a much higher level of complexity. However, while parametric design approaches have popularized the production of highly customized surfaces, the ability to realize these surfaces at reasonable costs without compromising the design intent remains a fundamental challenge (Eigensatz et al., 2010).

This fundamental issue, referred to as rationalization (Austern et al., 2018; Eigensatz et al., 2010), is largely concerned with panelization—defined as the division of a shape into simpler surface sections that can be manufactured cost-effectively using the selected production process (Eigensatz et al., 2010; Fu et al., 2010; Liu et al., 2024). While relying on a single type of panel tends to fall short of design objectives, the inclusion of a wide variety of curved elements increases fabrication complexity and often limits opportunities for mould reuse, thereby significantly increasing production costs (Eigensatz et al., 2010). Beyond the geometric rationalization of façade surfaces, minimizing the external envelope area relative to internal volume has been shown to reduce both thermal transfer and the embodied energy associated with cladding materials, without compromising usable space—a consideration of significant consequence for sustainable building design (D'Amico & Pomponi, 2019). Early-stage design decisions play a significant role because they influence approximately 80% of subsequent design phases (Bianchi et al., 2024). A review of the existing literature on how free-form geometries are addressed in early design phases reveals that energy efficiency, daylighting, environmental performance, and optimization are prominent research topics. For example, façade performance optimization has been examined in terms of energy consumption, visual comfort, and early-stage design decision-making processes (Hinkle et al., 2022; Mahdavinejad et al., 2024), while generative workflows have been proposed to support façade layout generation and geometric design exploration (B. Wang et al., 2025). In parallel, machine learning techniques have been increasingly adopted to reduce the computational burden of simulation-based design processes by enabling rapid performance prediction and design space exploration (C. Deb et al., 2021; Pham et al., 2020).

Machine learning techniques are used in various fields of architecture, such as computational design, façade design, building performance, and digital fabrication (Topuz & Çakici Alp, 2023). Most current studies focus on building performance, the optimization of facade arrangements, or energy-related objectives. Evaluating a large number of design alternatives—particularly in free-form structures where geometric complexity extends simulation times—remains a significant challenge. To overcome this limitation, data-driven approaches are being used throughout the design process to accelerate design evaluation and support decision-making. In particular, artificial intelligence (AI) is increasingly used for prediction, analysis, and design support in research (Duran et al., 2025). Among the various branches of artificial intelligence, machine learning has emerged as a powerful data-driven approach that enables systems to learn patterns from existing datasets and make predictions without being explicitly programmed for every scenario (Sarker, 2021). Machine learning-based surrogate models offer a promising solution by predicting performance outcomes from pre-existing simulation datasets, thereby reducing the need for computationally intensive simulation processes (Araújo et al., 2023). However, the integration of surrogate modelling with the geometric rationalization of complex free-form façade systems has received limited attention in the literature. In particular, there has been insufficient focus on the combined evaluation of geometric efficiency, panel standardization, and computational speed within a single workflow. Consequently, there is a need for computational approaches capable of addressing both geometric rationalization and efficient design space exploration in free-form architectural façades.

Building on the identified research gap, this study investigates whether an integrated workflow combining parametric modelling, evolutionary optimization and artificial neural network (ANN)-based surrogate modelling can improve geometric efficiency and panel standardization, while reducing the computational burden of free-form façade optimization. To evaluate this method, the Rhike Park Music Theatre and Exhibition Hall has been selected as a case study.

1.2 Case Study

The selected case study, designed by Massimiliano and Doriana Fuksas and completed in 2016 in Tbilisi, Georgia, presents a compelling example of a highly complex free-form structure (Figure 1). Formally, it consists of two tubular volumes with double curvature that converge at a shared retaining wall. This configuration introduces regions of variable Gaussian curvature, which are associated with geometric and fabrication challenges widely discussed in the literature on free-form surface design (Pottmann et al., 2007; H. Wang et al., 2019). The façade is entirely clad in stainless steel panels, mostly with non-repeating geometries; this further increases manufacturing complexity and production cost due to the need for different moulds for each panel (Castañeda et al., 2015; Eigensatz et al., 2010).

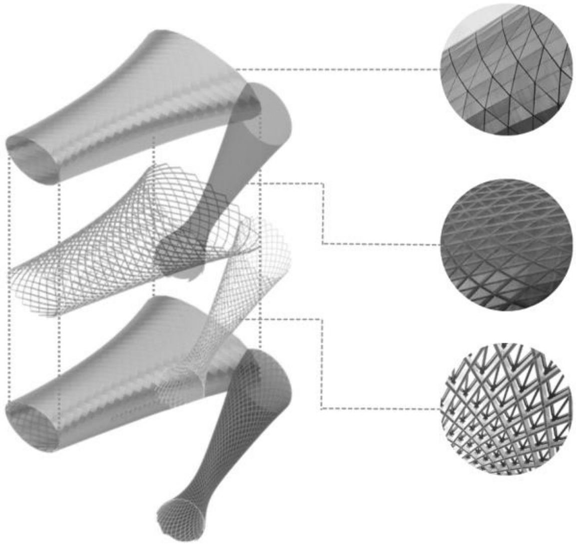

Figure 1. Rhike Park Axonometric Model: Illustration of the Diagrid System and Façade Cladding Layers.

In addition to these manufacturing challenges, the building's form creates significant complexity in the panelization process. Diamond-shaped panel systems present additional geometric challenges, particularly in meeting planar surface constraints and maintaining consistency between adjacent panels (Pottmann et al., 2007). These challenges become more pronounced in double-curved geometries, where maintaining geometric continuity across the surface is inherently complex. Consequently, such conditions may lead to geometric inconsistencies and visible façade irregularities. The intersection zone between the two volumes further compounds these challenges. By concentrating geometric variation within a limited region, this transition area increases the difficulty of maintaining geometric continuity across the surface —a challenge widely associated with the realisation of complex free-form structures (Eigensatz et al., 2010; Flöry & Pottmann, 2010; Pottmann et al., 2007). For these reasons, the Rhike Park Music Theatre was selected as a representative case study for this research. Its highly complex double-curved geometry, non-standardized façade panels, and fabrication challenges provide a suitable benchmark for evaluating computational rationalization and optimization strategies in free-form architectural envelopes.

When these challenges are considered as a whole, the limitations of traditional panelization methods become apparent, highlighting the need for optimization strategies that can enhance geometric efficiency, panel standardization, and manufacturability while preserving the architectural intent of the original design.

2. Materials and Methods

The workflow developed in this study consists of five stages. The process began with the reconstruction of the selected structure's form within the Rhino/Grasshopper environment; it then continued with form rationalization to make the original geometry more feasible. Subsequently, panelling was carried out through surface decomposition and the evaluation of panel configurations, leading to the search for an optimal panel solution. Given the observed computational constraints, a surrogate-based performance evaluation approach was developed to reduce simulation costs and accelerate design space exploration, utilizing a multi-layer perceptron (MLP)-based machine learning model trained on a dataset generated via Latin Hypercube Sampling (LHS). Consequently, a holistic approach has been adopted to rationalize free-form façades through the integration of optimization and data-driven modelling (Figure 2).

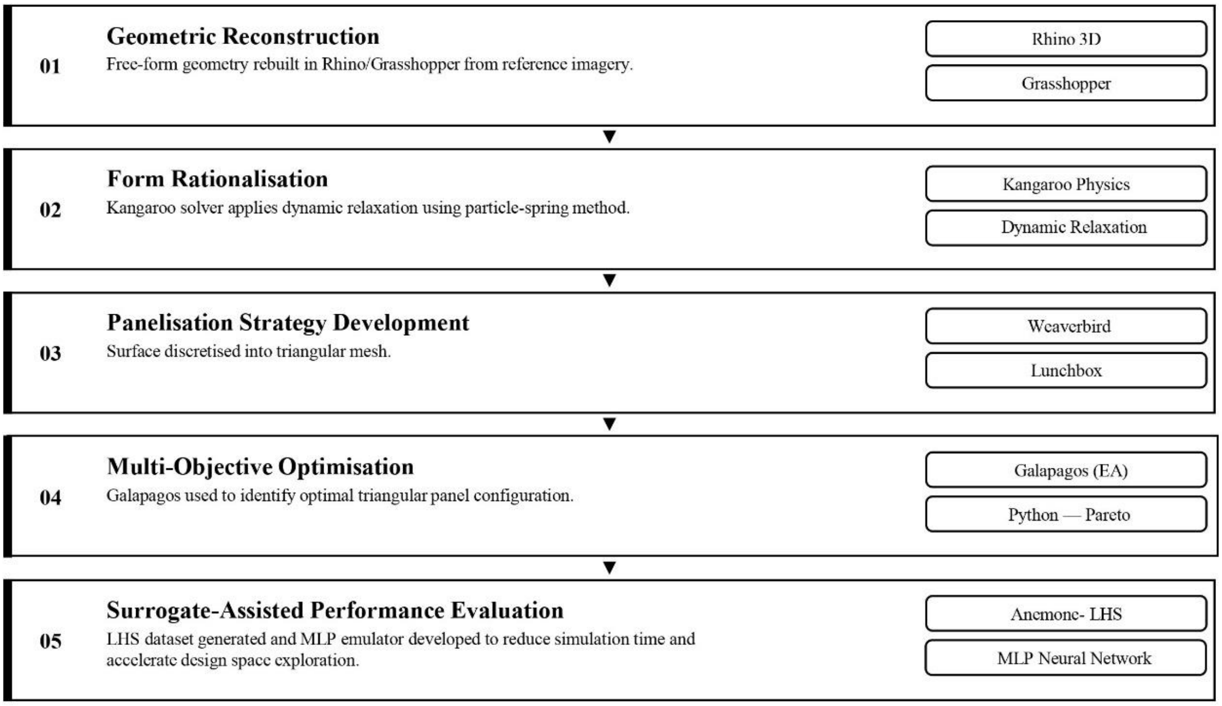

Figure 2. Structure of the Study.

To examine different geometric configurations throughout the optimization process, several design parameters were defined. These parameters were used in both the form rationalization and panelization stages and were selected based on preliminary tests to ensure sufficient geometric diversity while preserving the architectural characteristics of the original structure. Table 1 summarizes the optimization parameters, their ranges, and their roles within the workflow.

Table 1: Input and Output Variables Used in the Optimization Workflow.

Type	Variable	Symbol	Range / Objective	Rationale
Input	Length Factor	LF	0.40–0.70	Controls mesh relaxation behavior and geometric deformation during form rationalization.
Input	TriMesh Edge Length	x_0	2.00–4.00 m	Controls panel size, mesh density, and geometric resolution.
Output	Area Ratio	A_{Ratio}	Minimize	Measures the reduction of façade surface area relative to the original geometry.
Output	Volume Ratio	V_{Ratio}	Maximise	Measures the preservation of enclosed volume relative to the original geometry.

2.1 Geometric modelling and panelization workflow

2.1.1 Physics-based form finding

At this stage, the structure's free-form geometry was recreated in a digital environment. Rhino and Grasshopper were used to redefine the structure's form, and a physics-based form-finding method was applied using the Kangaroo plugin to achieve a fluid and balanced geometry. Kangaroo Physics, which is based on principles of dynamic relaxation and particle-based simulation, was used for the form-finding process in this study (Senatore & Piker, 2015). This method allowed the surface to evolve according to principles of tension and equilibrium, rather than through manual modelling (Figure 3).

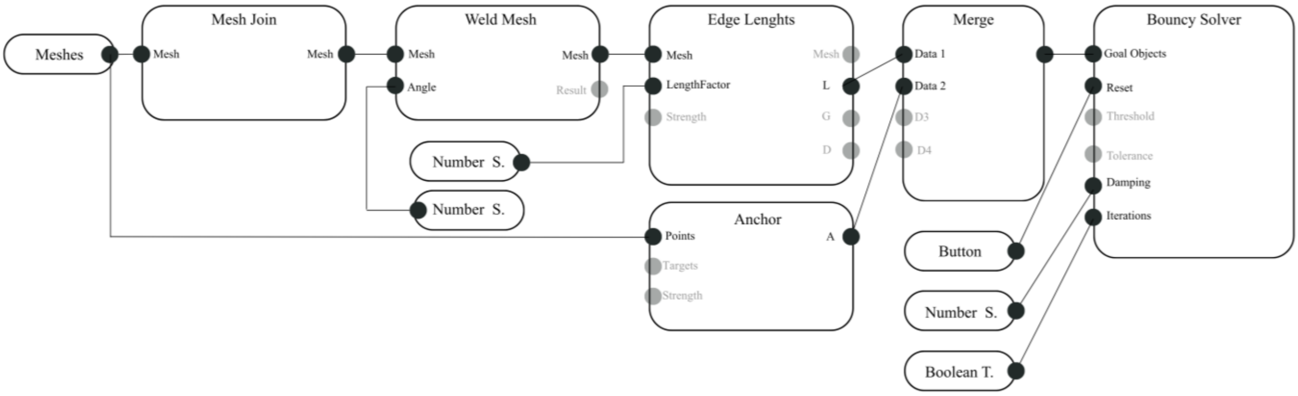

Figure 3. Grasshopper Tree Connections of Finding the Form through Kangaroo Solver.

Particle–spring systems are numerical methods in which nodal points are connected through spring-like elements, and the equilibrium configuration is obtained iteratively under applied forces and constraints (Alic & Persson, 2016). The dynamic relaxation technique is used extensively in calculating the equilibrium states of structures (Barnes, 1999) (Figure 4).

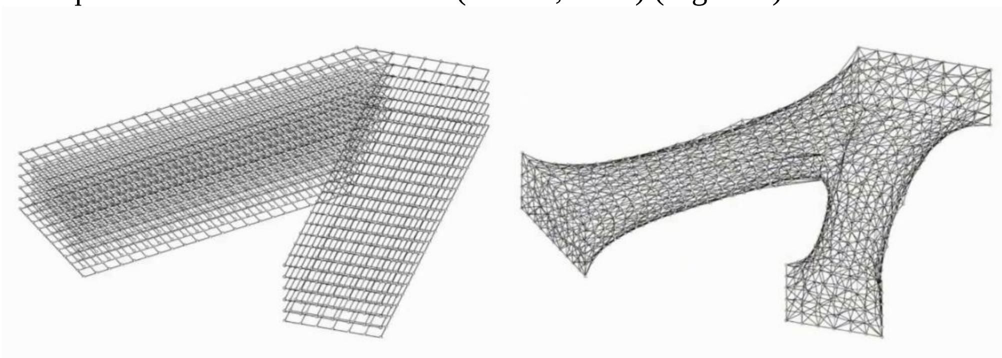

Figure 4. Kangaroo Mesh Relaxation.

The relaxation process was controlled using the Length Factor (LF) parameter, which determines the target length based on the initial states of the mesh edges (Figure 5). Preliminary tests showed that values below 0.4 led to excessive shrinkage and significant volume loss, whereas values above 0.7 resulted in only minor geometric changes and limited shape conformity. Therefore, the parameter range was limited to 0.4–0.7 to provide meaningful geometric variation while preserving the general characteristics of the original structure. For the initial form-finding stage, a representative LF value of 0.6 and a damping value of 14 were adopted in the Kangaroo Bouncy Solver. The resulting geometry was evaluated based on three criteria: preservation of the original building volume, surface continuity and smoothness, and preservation of the overall architectural form. This ensured that the geometry remained faithful to the architectural intent of the original design and established a suitable foundation for subsequent stages.

The existing diamond panel system was tested digitally using Grasshopper and Lunchbox. However, geometric continuity and panel consistency problems were observed on double-curved surfaces, leading to the adoption of a triangular panel system. The triangular configuration demonstrated improved geometric compatibility with the complex surface geometry and produced a more consistent panel layout. Consequently, it was used as the basis for the subsequent optimization process.

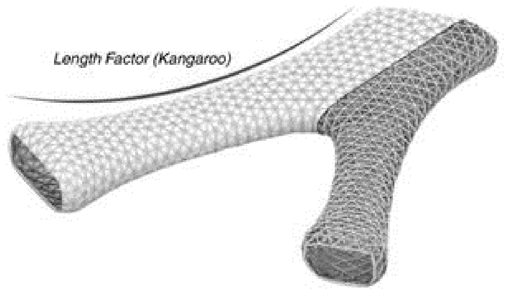

Figure 5. Length Factor Parameter.

2.2 Façade Optimization

The optimization of the façade design comprises four main phases. In the initial phase, a parametric model was created using the Weaverbird plugin in Grasshopper, and the surface was divided into triangular panels to obtain a more manufacturable geometry. In the second stage, different parameter combinations were tested using the Galapagos plugin to reduce the total surface area and minimize panel variety. In this way, solutions that optimize material usage were investigated. In the third stage, the parameter space was systematically explored to generate performance-related data for further analysis. This enabled the generation of performance data corresponding to different parameter combinations. In the final stage, the resulting dataset was transferred to the Python environment, where a lightweight predictive model was developed. This model enabled more efficient exploration of the design space by allowing performance outputs to be predicted rapidly without rerunning the geometric calculations.

2.2.1 Panel geometry optimization

This section focuses on generating and refining a new panel geometry to improve constructability and support subsequent optimization.

Initially, a diamond panel pattern was tested to match the existing façade character. However, during its application to double-curved surfaces, various issues arose regarding panel continuity, planarity, and installation. Therefore, a transition to a triangular panel system was made to achieve a more stable, manufacturable solution. This change simplified joint details, improved panel alignment, and resulted in a more consistent surface organisation, particularly in curved areas.

The triangular panel system enabled a more stable and manufacturable façade geometry while allowing parametric control over panel density and frame dimensions.

2.2.2 Search for optimal solutions

The Galapagos plugin in Grasshopper was used to identify optimal solutions for the generated panel geometry. Two primary design variables were used in the optimization: TriMesh Length [x_0] and Face Count [x_1]. While TriMesh Length controls the edge length of the initial triangular mesh subdivision, Face Count determines the target number of faces on the reduced mesh (Figure 6).

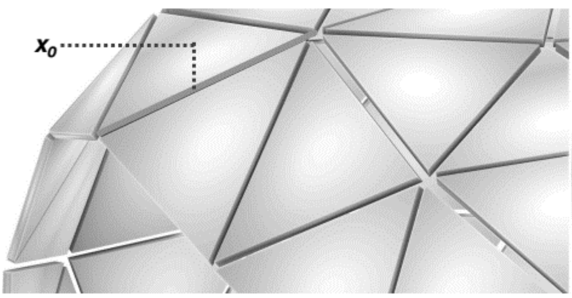

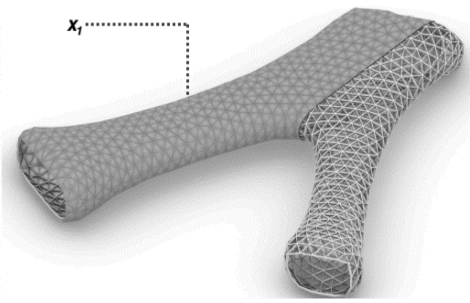

Figure 6. Design Variables [x0, x1]-Trimesh Length (left) and Total Number of Panels (right).

The parameter ranges were determined through preliminary experiments to ensure sufficient geometric diversity. While low TriMesh Length values resulted in overly dense meshes, thereby increasing computational costs, high values reduced geometric accuracy. Similarly, the selected Face Count range struck a balance between panel standardization and geometric accuracy. During the optimization process, an attempt was made to minimize two conflicting objectives simultaneously: reducing the number of unique panel types and minimizing the total surface area. Since Galapagos operates on a single-objective optimization logic, these two objectives were combined into a weighted fitness function. For the first objective, unique panel standardization, the mesh surface polylines were extracted using Weaverbird and classified based on size and shape similarities via a Python script. The resulting count of unique panel types was then normalized to ensure comparability across different configurations, using the following method:

$$F_1 = \frac{C_{unique} - C_{min}}{C_{max} - C_{min}} \quad (1)$$

where F_1 represents the normalized unique panel count, C_{unique} is the number of unique panel types in the current solution, and C_{min} and C_{max} are the minimum and maximum unique panel counts observed across all tested configurations.

The second objective, total material area, was calculated based on the final panel geometry generated using the Weaverbird Mesh Thicken component and normalized as follows:

$$F_2 = \frac{A_{total} - A_{min}}{A_{max} - A_{min}} \quad (2)$$

where F_2 represents the normalized material area, A_{total} is the total computed area of the generated panel system, and A_{min} and A_{max} are the minimum and maximum area values obtained during the optimization process. These two objectives were combined using the following weighted fitness function:

$$F_{total} = (w_1 \cdot F_1) + (w_2 \cdot F_2) \quad (3)$$

where w_1 and w_2 are the weighting coefficients assigned to each objective. In this study, equal weighting was adopted ($w_1 = 0.50\,, w_2 = 0.50$) to assign the same level of importance to both objectives during optimization. The process generated numerous alternatives with the aim of minimizing this composite fitness score, and the resulting data was subsequently used for Pareto analysis and surrogate model training. Since the optimization involved two conflicting objectives, the resulting solution set was further evaluated using Pareto analysis to identify balanced design alternatives. Solutions located on the Pareto front are considered non-dominated, meaning that any attempt to enhance performance in one objective inevitably leads to a trade-off, or reduction, in at least one of the remaining objectives (K. Deb, 2011; Gunantara, 2018).

Reducing the total surface area and reducing the number of unique panel types are conflicting objectives. Therefore, rather than a single optimal solution, Pareto-optimal solutions that balance these objectives were examined. Data obtained from the Galapagos optimization algorithm were imported into Excel and analyzed using Python. The Pareto front illustrates the boundary region where improving one objective worsens the other (Figure 7).

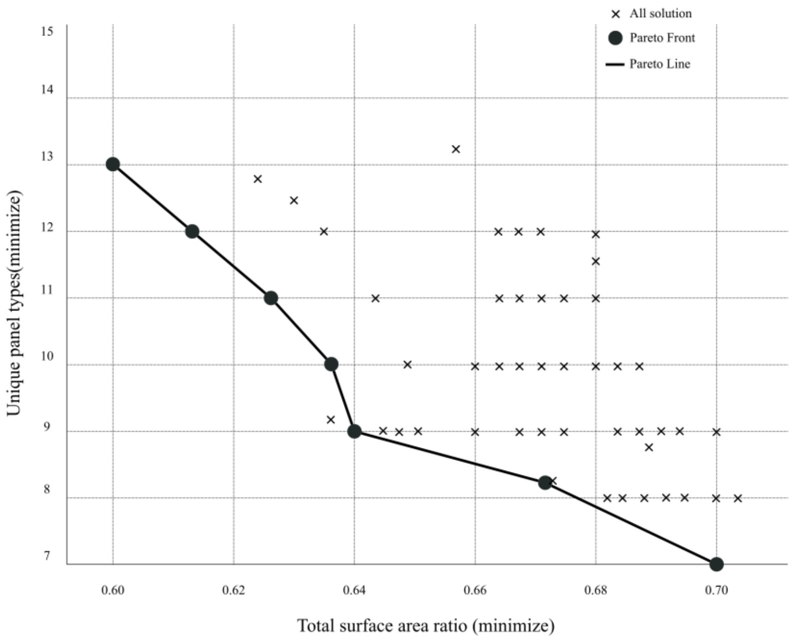

Figure 7. Pareto Front Analysis.

The analysis shows that solutions on the left side of the curve result in lower material use but require more panel types, increasing production and assembly complexity. In contrast, solutions on the right side of the curve improve panel standardization and constructability by reducing the number of unique panel types, but this comes at the cost of increased material usage. A notable inflection point is observed near the center of the curve, indicating a balanced region where relatively small increases in material usage lead to significant reductions in manufacturing complexity. Therefore, this region can be considered the most efficient compromise between material efficiency and constructability. Table 2 presents the Pareto-optimal solutions identified during the optimization process and illustrates the trade-off between surface area ratio and panel standardization.

Table 2: Trade-off Analysis: Surface Area Ratio versus Panel Standardization Across Pareto-Optimal Solutions.

Mesh length	Number of panels	Total surface area ratio	Unique types	Pareto
4.00	1883	0.595	13	TRUE
3.95	1818	0.615	12	TRUE
3.93	1769	0.625	11	TRUE
3.80	1943	0.637	10	TRUE
3.76	1759	0.640	9	TRUE
3.24	1982	0.670	8	TRUE
2.86	1949	0.695	7	TRUE

However, since the optimization process took up to 10 hours to complete the simulation, saving energy and time was quite labor-intensive. This limitation highlighted the inefficiency of relying solely on iterative optimization and prompted the search for a more time-efficient, data-driven approach to explore a broader design space.

2.3 Dataset generation and parameter space exploration

Following the constraints observed during the direct optimization process, a more comprehensive dataset was created to systematically explore the parameter space and support proxy model development efforts. At this stage, the key control parameters influencing geometric behaviour and performance metrics were identified, and meaningful value ranges were defined based on preliminary Grasshopper tests.

The first parameter, the Length Factor (LF), determines the target length of each network edge based on its initial state. The parameter was restricted to the range of 0.4–0.7, as determined by preliminary tests.

The second key parameter used in this study is the TriMesh Edge Length, which determines the triangular mesh resolution on the surface (Figure 8). TriMesh Edge Length controls mesh resolution and panel density across the surface.

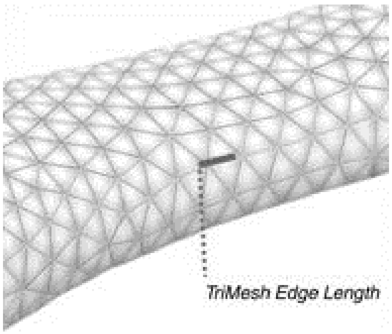

Figure 8. TriMesh Edge Length Parameter.

The TriMesh Edge Length parameter is not a variable that directly defines the area (A) and volume (V) outputs, but when used in conjunction with the form finding process, it has an indirect yet systematic effect on these outputs. Since equilibrium is solved iteratively through nodal force interactions in dynamic relaxation methods, changes in mesh resolution affect deformation distribution and convergence behaviour (Barnes, 1999).

In this study, the TriMesh Edge Length was maintained within the range of 2–4, to analyse the effects of different densities on area and volume, along with their panelization behaviour. The selected range was determined to ensure that the panel dimensions of the geometry remain within an easily producible range, while also allowing the resulting geometric differences to be observed. In this context, the Length Factor is a complementary parameter that defines the physics-based deformation behaviour of the surface, while the TriMesh Edge Length defines how this deformation is numerically solved and at what level of resolution the surface is represented. The joint evaluation of these two parameters enables a systematic analysis of their effects on outputs such as area and volume, in addition to the panelization behaviour.

Using these two parameters, a structured sampling method was applied to generate a representative dataset within the defined design space.

2.3.1 Sampling method: Latin Hypercube Sampling (LHS)

After determining the main control parameters and their valid ranges, the next step was to systematically map the design space and construct a representative dataset. For this purpose, the Latin Hypercube Sampling (LHS) method was used, in which each variable range is divided into segments of equal probability and one sample is drawn from each segment; this is a stratified approach commonly used for design space sampling (Chen, 2024; Freimer et al., 2012; McKay et al., 1979). In this study, the predefined two-dimensional parameter space consists of the Length Factor and TriMesh Edge Length, with each sample representing a unique combination of these variables. This approach ensures a more homogeneous distribution of samples across the design space compared to fully random sampling. Furthermore, as the predictive accuracy of surrogate models depends to a large extent on the quality and information content of the training data, it is crucial to select an appropriate sampling strategy in order to create reliable surrogate models (Mehrotra & Yi, 2023). A total of 500 sampling points were generated for the two selected design variables. Since surrogate-based building performance studies commonly employ simulation datasets ranging from several hundred to around one thousand cases, depending on how many variables were involved and how intricate the design space was, this sample size was deemed appropriate given the study's objectives (Hinkle et al., 2022; Westermann & Evins, 2019). Additionally, several different sample sizes were tested during preliminary experiments, and 500 samples yielded the most accurate and stable emulator performance. To enable the testing of different sampling strategies within a parametric workflow, the Latin Hypercube Sampling algorithm was integrated with the Python 3 component in the Grasshopper environment. This script was designed to operate in both simplified and fully independent sampling scenarios via a user-defined mode parameter.

To ensure that each sampled parameter combination produced a stable form rather than merely generating input values, the Anemone plugin was used in Grasshopper. Anemone was used to iteratively evaluate each parameter combination until geometric equilibrium was reached (Figure 9).

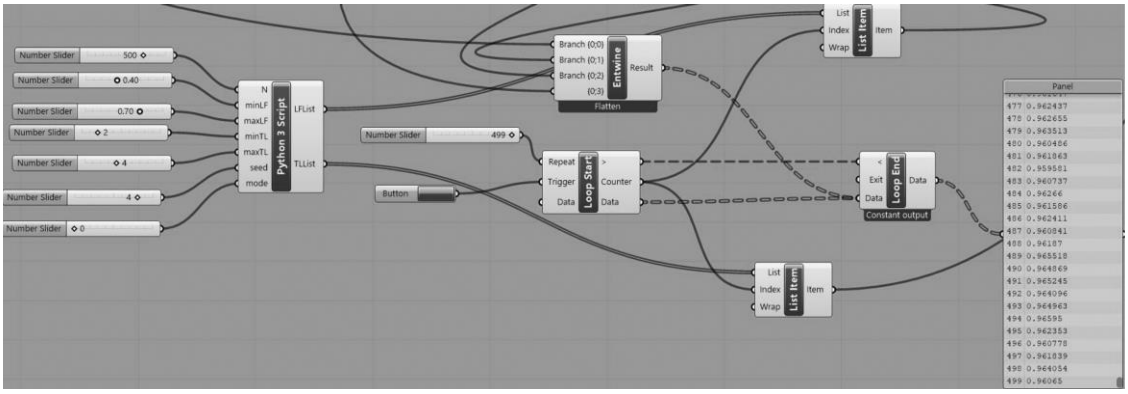

Figure 9. Grasshopper Data Sampling and Anemone Loop.

In this study, Anemone was used to repeatedly evaluate each Length Factor–TriMesh Edge Length combination throughout the form-finding process. For each sampled input, the intermediate geometries generated by Kangaroo Physics were continuously updated until the system approached equilibrium. As a result, each sampling point was represented not by a single-step geometric output, but by a stable geometry obtained through an iterative simulation process.

2.3.2 Output Metrics and Normalisation

Two output metrics were calculated to evaluate the geometric behaviour of each sampled configuration: total surface area (A) and enclosed volume (V). These metrics were selected because surface area correlates closely with how much material is used and the efficiency of the outer shell. At the same time, the enclosed volume represents the spatial capacity of the generated form. Since the surface-to-volume proportion influences the compactness level of the form and its potential heat exchange with the external environment, these two outputs were considered suitable indicators for comparing the generated geometries (Bekkouche et al., 2013).

To ensure direct comparability between outputs from different parameter combinations, the calculated values were normalized to the initial geometry of the structure. The normalisation process for each output metric is defined as follows:

$$A_{Ratio} = \frac{A_i}{A_0} \tag{4}$$

$$V_{Ratio} = \frac{V_i}{V_0} \tag{5}$$

where A_i and V_i represent the surface area and enclosed volume of the sampled configuration, and A_0 and V_0 represent those of the initial geometry.

2.4 Surrogate model development and evaluation

A surrogate model—also known as an emulator or metamodeling—is a computationally efficient approximation constructed using data generated from a high-fidelity simulation model to provide rapid predictions of its outputs (Queipo et al., 2005). In this study, the emulator aimed to provide a more effective alternative to the iterative simulation model developed in Grasshopper, thereby enabling the rapid evaluation of alternative design configurations during the optimization process. Based on a previously created dataset, the emulator was trained using two input variables and two output variables. The selected input variables were the Length Factor (LF) and TriMesh Edge Length, which represent the fundamental deformation and discretization parameters within the parametric workflow. The emulator estimated the Area Ratio and Volume Ratio from the normalized simulation results. By learning the relationship between these input and output variables, the emulator provided a simplified yet reliable representation of the simulation model for subsequent optimization and design space exploration tasks.

2.4.1 Emulator training and validation

After creating a representative dataset through data sampling and iterative simulation, a surrogate modelling method was employed to process this data and enable faster prediction of performance outcomes in the optimization process. To this end, a supervised regression emulator was developed using a multi-layer perceptron (MLP), a type of artificial neural network (ANN), to approximate the nonlinear relationship between the selected design inputs and performance outputs based on input–output data (Jahirul et al., 2021; Meng & Karniadakis, 2020; Yang et al., 2023). ANNs are computational models that learn complex nonlinear mappings through interconnected processing layers and are widely used in performance prediction studies involving surrogate modelling (Afzal et al., 2017; Hornik et al., 1989).

In this study, an ANN architecture comprising an input layer, two hidden layers containing 100 and 50 neurons, and an output layer was used to develop a surrogate model. While the input layer received the selected design variables (Length Factor and TriMesh Edge Length), the output layer predicted the target geometric performance values (Area Ratio and Volume Ratio) (Figure 10).

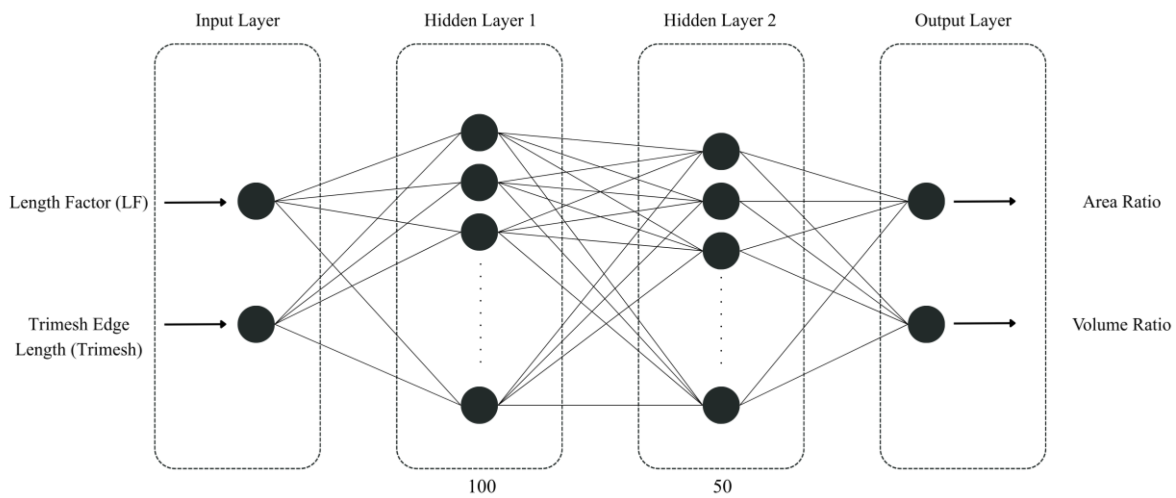

Figure 10. Structure of the Artificial Neural Network (ANN) Emulator used in this study.

The ReLU activation function was used to capture the nonlinear relationships in the dataset. Model training was performed using the Adam optimizer, a gradient-based optimization algorithm widely used for efficient neural network training (Kingma & Ba, 2017), with a learning rate of 0.001 and the mean squared error (MSE) as the loss function. The dataset consisted of 500 samples generated from a simulation workflow in Grasshopper. The dataset was split into training and test subsets in an 80:20 ratio; 80 per cent of the samples were used for model training, whilst the remaining 20 per cent were set aside for testing. Before training, all input and output variables were standardized using z-score normalisation to improve convergence and prevent scale dominance during optimization. Training was performed iteratively until convergence, with a predefined maximum number of epochs to prevent overfitting. Model performance was assessed through a set of regression-based evaluation criteria, including R^2, MAE, and RMSE. While R^2 was used to assess how well the emulator captured the variation and overall trend in the simulation results, MAE and RMSE were used as complementary error metrics. MAE measures the average absolute difference between the reference values and the predicted values, while RMSE is calculated as the square root of the mean squared error and expresses the error in the same units as the target variable (Chicco et al., 2021; Hodson, 2022).

2.4.2 Emulator-based optimization

Following the training and validation, a neural network emulator was used in place of the original Grasshopper-based workflow to perform rapid design-space exploration and optimization. A dense grid of input parameter combinations was created within the boundaries of the original dataset, covering the full range of Length Factor (LF) and TriMesh Edge Length values used during data collection. The trained emulator was used to rapidly evaluate thousands of parameter combinations and identify optimal solutions based on area and volume performance. For each combination, the emulator estimated the corresponding Area and Volume outputs; this made it possible to evaluate thousands of solutions in a negligible amount of time compared to iterative parametric simulation. These outputs were combined into a single performance score to define a scalar objective function.

3. Results

3.1 Comparison of optimization methods

To evaluate the effectiveness of different optimization techniques, the baseline model, the model generated with Galapagos, and the model generated with an emulator were compared in terms of geometric performance, shell properties, and computation time.

The model optimized with Galapagos was obtained directly via an evolutionary search. A total of 2,253 panels were generated in this model; although this resulted in a denser panelization pattern than in the emulator model, it still achieved the target. However, due to the nature of the simulation-based model, the analysis took approximately 10 hours to complete. As shown in Figure 11, panel areas in the Galapagos model were concentrated within a limited range, whereas the emulator-generated results showed a more balanced distribution across various panel sizes. This indicates a more homogeneous panel distribution and a reduction in the excessive clustering of panel sizes.

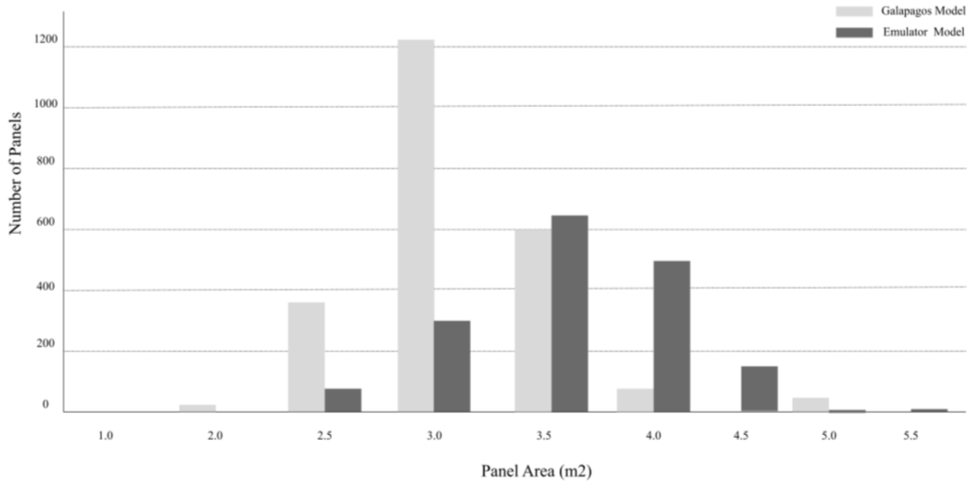

Figure 11. Panel Area Distribution.

Table 3: Comparison of Galapagos and Emulator-Based Optimization Results.

Metric	Galapagos Model	Emulator Model
Total Panel Count	2,253	1,669
Computation Time	~10 hours	~5 seconds

As shown in Table 3, the emulator model reduced the total number of panels by approximately 26% while cutting the computation time from about 10 hours to 5 seconds. Although both approaches yielded similar results in terms of area and volume, the emulator enabled a much faster exploration of the design space, allowing for the evaluation of more design alternatives in a much shorter time.

3.2 Geometric performance evaluation

The final design achieved a reduction of approximately 40% in surface area while retaining 95% of the original volume. In other words, material efficiency was increased while preserving the building's spatial capacity. The results obtained are consistent with previous studies that emphasize the importance of building geometry as a fundamental design variable and highlight the optimization potential of shape modifications in improving building performance (Kistelegdi et al., 2022). Therefore, the results of this study point to a more efficient geometric configuration.

3.3 Panelization performance analysis

The number of panels and the distribution of panel sizes on the surface after panelization were analyzed with respect to panel standardization and repeatability, which are important for production efficiency. Panel areas were classified into predefined ranges to evaluate panel standardization and repeatability (Figure 12). The resulting area data was transferred to Python and classified using a user-defined step size. This step size determines the precision with which panel dimensions are grouped and directly affects the classification resolution.

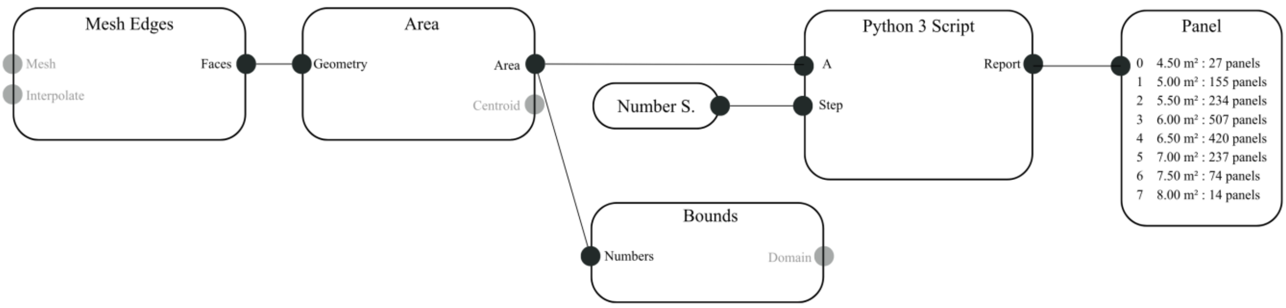

Figure 12. Calculation of Unique Panel Classes in Grasshopper.

This classification is based on the principle of rounding each panel area to the nearest class according to the selected step interval and is expressed by Equation (6).

$$k_i = round\ (\frac{A_i}{\Delta}) \cdot \Delta \tag{6}$$

In Equation (6), A_i represents the area of the relevant panel; Δ represents the step size defined by the user; and k_i represents the area class to which the panel belongs. Following this classification, the number of panels assigned to each area class was calculated using Equation (7).

$$n(k) = |\{i \mid k_i = k\}| \tag{7}$$

The greatest challenge in free-form architecture stems from irregularly shaped panels; because each panel is different from the others, this eliminates the possibility of repetition and increases costs (Gołębiowska, 2025). The optimization process reduced the number of unique panel classes from 18 to 8, indicating improved standardization (Table 4).

Table 4: Comparison of Unique Panel Types Before and After Optimization.

Panel Area Range (m^2)	Before Optimization	After Optimization
2.0 – 3.5	588	0
4.0 – 5.5	548	420
6.0 – 7.5	316	1326
8.0+	230	14
Model	Number of Unique Panels	Reduction (%)
Initial Model	18	—
Optimized Model	8	55.6% ↓

In addition, to evaluate panel dimensions for manufacturability—since panel size directly affects material usage, processing time, and production efficiency (Austern et al., 2018)─an appropriate range of panel areas has been established. Accordingly, in the Grasshopper environment, panels within the defined optimal range are displayed in green. In contrast, panels exceeding this range are shown with a color gradient from yellow to red, indicating an increasing likelihood of manufacturability issues (Figure 13).

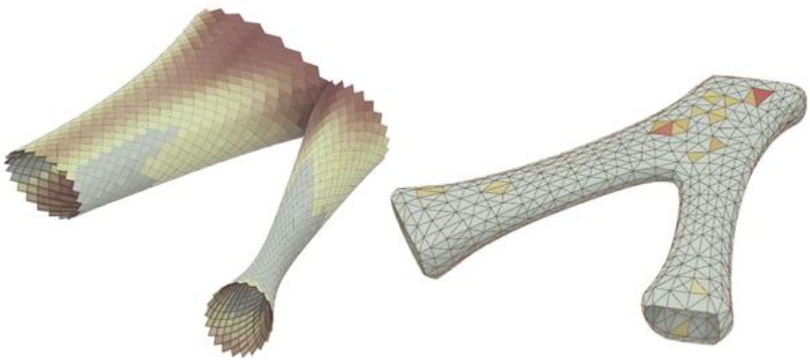

Figure 13. Panel Size Distribution: Baseline versus Optimized Model.

A comparison between the initial and optimized models clearly shows that the optimization process narrowed the distribution of panel sizes and reduced the number of unique panels, resulting in a more standardized and manufacturable panel system.

3.4 Emulator results

This section presents the neural network emulator's performance and the results of the optimization process. Figure 14 shows comparison plots that contrast the emulator-predicted values with the Area and Volume reference values generated by Grasshopper. Each plot includes an ideal 1:1 reference line, allowing for a direct visual assessment of prediction accuracy.

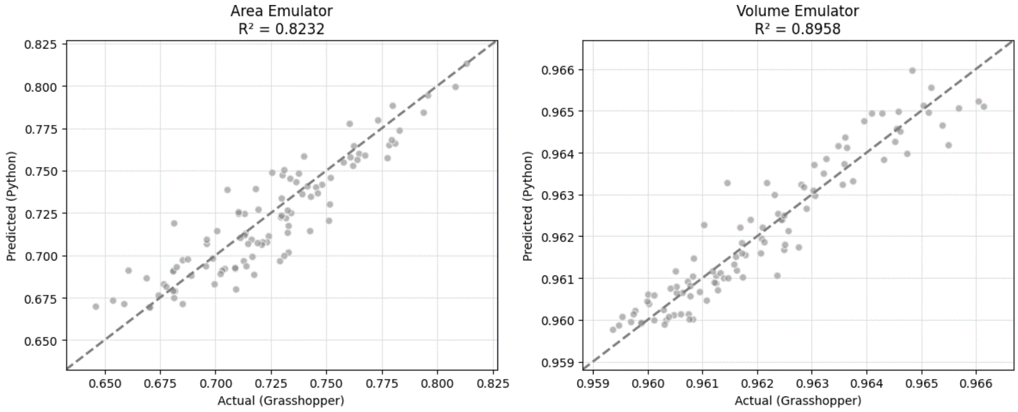

Figure 14. Comparison of Predicted and Reference Values for Area and Volume.

For both outputs, the predicted values closely follow the diagonal line, indicating good agreement between the emulator and the original parametric model. The distribution of the data points remains confined within the evaluated range, and no significant systematic bias is observed. The tighter clustering observed for Volume indicates stronger predictability from the selected input parameters, while Area maintains a distinct linear trend but shows slightly greater dispersion.

The neural network emulator has achieved satisfactory prediction accuracy for both outputs; the R^2 values for Area are above 0.80, while those for Volume are close to 0.90. Low MAE and RMSE values confirm that deviations between the emulator predictions and the Grasshopper reference values remained limited throughout the evaluated range (Table 5).

Table 5: Performance Metrics of the Neural Network Emulator

Output	R^2	MAE	RMSE
Area	0.8232	0.0121	0.0149
Volume	0.8958	0.0004	0.0006

Between the two outputs, Volume demonstrated stronger predictive performance, as evidenced by a higher R^2 and lower errors. This indicated that Volume was more directly influenced by the selected input parameters, resulting in a smoother and more trainable response surface. Although the area estimates exhibited greater variability, they remained within acceptable limits.

To examine the optimization potential of the trained emulator in greater detail, the top five candidate input combinations identified in the emulator model are presented in Table 6.

Table 6: Top 5 Optimal LF–TriMesh Combinations

Rank	LF	TriMesh	Score	Area	Volume
1	0.400142	1.028427	1.620543	0.661157	0.959386
2	0.401649	1.028427	1.620578	0.661179	0.959399
3	0.403155	1.028427	1.620609	0.661197	0.959411
4	0.404662	1.028427	1.620637	0.661213	0.959424
5	0.406168	1.028427	1.620665	0.661228	0.959436

The results are clustered in a narrow area of the parameter space where the solutions exhibit the best performance, indicating a consistent relationship between the input parameters and geometric performance. The distribution of the optimization score within the LF–TriMesh parameter space was examined using a contour plot. Lower score values, indicated by blue and green regions, represent more favorable design solutions, whereas higher values, shown in yellow regions, correspond to less efficient configurations. A smooth, continuous response surface is observed, suggesting that the emulator captures the underlying behavior of the original model. Moreover, the identified optimal region confirms that specific combinations of LF and TriMesh consistently lead to improved geometric efficiency and allow intuitive interpretation of parameter sensitivities (Figure 15).

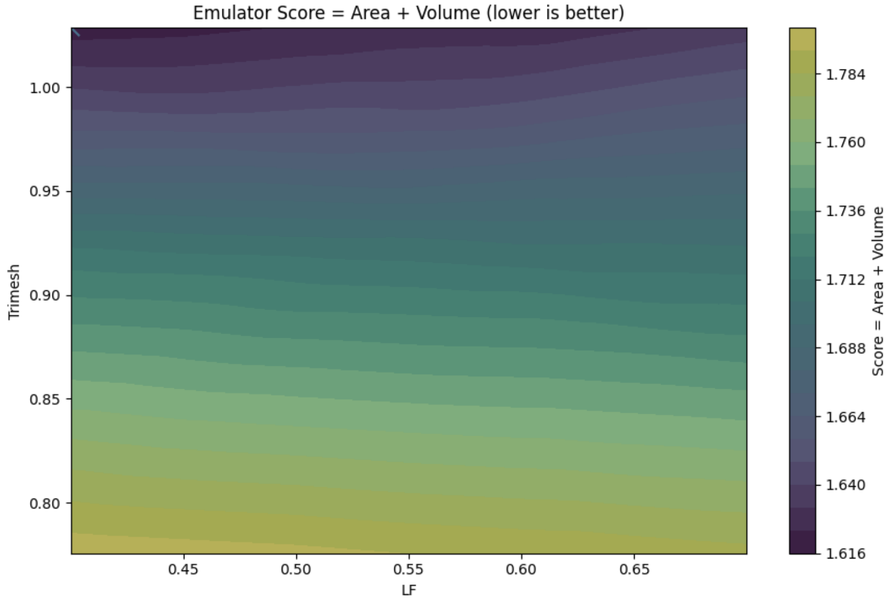

Figure 15. Contour Plot of Optimization Score.

4. Discussion

The results show that surrogate model-assisted optimization can significantly improve computational efficiency in rationalising free-form façade systems. Compared to direct evolutionary optimization, the surrogate model-based approach enabled much faster exploration of the parameter space while achieving geometric results that were either similar or better. This suggests that machine learning can be utilised as a decision-support tool in early-stage design. Moreover, the reduction in unique panel types from 18 to 8 indicates improved panel standardization, which can simplify fabrication and reduce costs, particularly in more geometrically complex free-form structures. However, this study has some limitations. The optimization process relies on only two design parameters, thereby limiting the representation of the full design space. Additionally, the slope variable was excluded due to its low correlation with the selected inputs and may require alternative evaluation methods in future studies.
In this study, only one machine learning method (ANN/MLP) was tested. Furthermore, the current framework focuses solely on geometric efficiency and manufacturability; structural performance, environmental impact, and cost analysis have not been included.

5. Conclusion

This study has demonstrated that computational optimization and surrogate modelling can effectively support the rationalization of complex free-form façade systems. Using the Rhike Park Music Theatre and Exhibition Hall as a case study, the proposed workflow reduced the surface area, the variety of panels, and the total number of panels while preserving most of the original volumetric capacity. The results show that the emulator-based optimization approach significantly reduces computation time while delivering geometric performance comparable to, or better than, that of direct evolutionary optimization. Thus, the practicality of machine learning-based surrogate models for rapid design space exploration and early-stage decision-making processes has been demonstrated. This study contributes to the literature by demonstrating the feasibility of surrogate modelling for the optimization of free-form architectural façades. Although surrogate modelling has been widely applied in performance-based optimization, its use in the rationalization of architectural façades remains limited. The proposed workflow facilitates a more efficient exploration of design alternatives by supporting early-stage design decisions while reducing the computational load and maintaining geometric performance.

Despite these contributions, the study has some limitations. The optimization process was limited to two geometric design parameters and focused solely on geometric rationalization. Structural behaviour, environmental performance, manufacturing constraints, and cost analysis were not included in the optimization framework. Furthermore, the proposed workflow was validated using a single case study, which may limit the generalizability of the findings to other free-form façade geometries.

Future research should expand the proposed framework by integrating structural, environmental, and cost analyses into the optimization process. The use of alternative surrogate modelling techniques, such as Gaussian process regression or random forests, could also be explored and compared with ANN/MLP models. Furthermore, validating the workflow by applying it to different free-form structures may enhance its robustness and scalability.

Acknowledgements

The author would like to thank Assistant Professor Dr. İmdat As for his valuable guidance and feedback throughout the process. The author also thanks Paul Badri, Tajdine El Maslouhi, and Nandhagopal Yuvaraj for their collaboration and support.

Funding

This research received no specific grant from any funding agency in the public, commercial, or not-for-profit sectors.

Conflicts of Interest

The author reports no conflicts of interest.

Data availability statement

The data and computational models used in this study are available from the corresponding author upon reasonable request.

Institutional Review Board Statement

Not applicable.

CRediT author statement

The author was responsible for conceptualization, methodology, data collection, software, visualization, writing—original draft, and writing—review and editing. The author has reviewed and approved the final version of the manuscript.

References

Afzal, A., Kim, K.-Y., & Seo, J. (2017). Effects of Latin hypercube sampling on surrogate modeling and optimization. *International Journal of Fluid Machinery and Systems*, *10*(3), 240–253. https://doi.org/10.5293/IJFMS.2017.10.3.240

Alic, V., & Persson, K. (2016). Form finding with dynamic relaxation and isogeometric membrane elements. *Computer Methods in Applied Mechanics and Engineering*, *300*, 734–747. https://doi.org/10.1016/j.cma.2015.12.009

Araújo, G. R., Gomes, R., Gomes, M. G., Guedes, M. C., & Ferrão, P. (2023). Surrogate Models for Efficient Multi-Objective Optimization of Building Performance. *Energies*, *16*(10), 4030. https://doi.org/10.3390/en16104030

Austern, G., Capeluto, I. G., & Grobman, Y. J. (2018). Rationalization methods in computer aided fabrication: A critical review. *Automation in Construction*, *90*, 281–293. https://doi.org/10.1016/j.autcon.2017.12.027

Barnes, M. R. (1999). Form Finding and Analysis of Tension Structures by Dynamic Relaxation. *International Journal of Space Structures, 14*(2), 89–104. https://doi.org/10.1260/0266351991494722

Bekkouche, S. M. A., Benouaz, T., Cherier, M. K., Hamdani, M., Yaiche, M. R., & Benamrane, N. (2013). Influence of the compactness index to increase the internal temperature of a building in Saharan climate. *Energy and Buildings*, *66*, 678–687. https://doi.org/10.1016/j.enbuild.2013.07.077

Bianchi, S., Andriotis, C., Klein, T., & Overend, M. (2024). Multi-criteria design methods in façade engineering: State-of-the-art and future trends. *Building and Environment*, *250*, 111184. https://doi.org/10.1016/j.buildenv.2024.111184

Castañeda, E., Lauret, B., Lirola, J. M., & Ovando, G. (2015). Free-form architectural envelopes: Digital processes opportunities of industrial production at a reasonable price. *Journal of Façade Design and Engineering*, *3*(1), 1–13. https://doi.org/10.3233/FDE-150031

Chen, X. (2024). *Enhancing Estimation and Uncertainty Quantification in Stochastic Optimization: Importance Sampling and Bootstrap Resampling* [PhD dissertation, University of California, Davis]. ProQuest Dissertations and Theses Global (Publication No. 31328967).

Chicco, D., Warrens, M. J., & Jurman, G. (2021). The coefficient of determination R-squared is more informative than SMAPE, MAE, MAPE, MSE and RMSE in regression analysis evaluation. *PeerJ Computer Science*, *7*, e623. https://doi.org/10.7717/peerj-cs.623

D’Amico, B., & Pomponi, F. (2019). A compactness measure of sustainable building forms. *Royal Society Open Science*, *6*(6), 181265. https://doi.org/10.1098/rsos.181265

Deb, C., Dai, Z., & Schlueter, A. (2021). A machine learning-based framework for cost-optimal building retrofit. *Applied Energy*, *294*, 116990. https://doi.org/10.1016/j.apenergy.2021.116990

Deb, K. (2011). Multi-Objective Optimization Using Evolutionary Algorithms: An Introduction. In L. Wang, A. H. C. Ng, & K. Deb (Eds), *Multi-objective evolutionary optimisation for product design and manufacturing* (pp. 3–34). Springer. https://doi.org/10.1007/978-0-85729-652-8_1

Duran, A., Waibel, C., Piccioni, V., Bickel, B., & Schlueter, A. (2025). A review on artificial intelligence applications for facades. *Building and Environment*, *269*, 112310. https://doi.org/10.1016/j.buildenv.2024.112310

Eigensatz, M., Kilian, M., Schiftner, A., Mitra, N. J., Pottmann, H., & Pauly, M. (2010). Paneling architectural freeform surfaces. *ACM SIGGRAPH 2010 Papers*, *29*(4), 1–10. https://doi.org/10.1145/1833349.1778782

Flöry, S., & Pottmann, H. (2010). Ruled Surfaces for Rationalization and Design in Architecture. *ACADIA 10: LIFE in:Formation: On Responsive Information and Variations in Architecture*, 103–109. https://doi.org/10.52842/conf.acadia.2010.103

Freimer, M. B., Linderoth, J. T., & Thomas, D. J. (2012). The impact of sampling methods on bias and variance in stochastic linear programs. *Computational Optimization and Applications*, *51*(1), 51–75. https://doi.org/10.1007/s10589-010-9322-x

Fu, C.-W., Lai, C.-F., He, Y., & Cohen-Or, D. (2010). K-set tilable surfaces. *ACM Transactions on Graphics*, *29*(4), 1–6. https://doi.org/10.1145/1778765.1778781

Gołębiowska, M. (2025). Optimizing Glass Panel Geometry for Freeform Architecture: A Curvature-Based Pavilion Study. *Buildings*, *15*(20), 3635. https://doi.org/10.3390/buildings15203635

Gunantara, N. (2018). A review of multi-objective optimization: Methods and its applications. *Cogent Engineering*, *5*(1), 1502242. https://doi.org/10.1080/23311916.2018.1502242

Hinkle, L. E., Wang, J., & Brown, N. C. (2022). Quantifying potential dynamic façade energy savings in early design using constrained optimization. *Building and Environment*, *221*, 109265. https://doi.org/10.1016/j.buildenv.2022.109265

Hodson, T. O. (2022). Root-mean-square error (RMSE) or mean absolute error (MAE): When to use them or not. *Geoscientific Model Development*, *15*(14), 5481–5487. https://doi.org/10.5194/gmd-15-5481-2022

Hornik, K., Stinchcombe, M. B., & White, H. (1989). Multilayer feedforward networks are universal approximators. *Neural Networks*, *2*(5), 359–366. https://doi.org/10.1016/0893-6080(89)90020-8

Jahirul, M. I., Rasul, M. G., Brown, R. J., Senadeera, W., Hosen, M. A., Haque, R., Saha, S. C., & Mahlia, T. M. I. (2021). Investigation of correlation between chemical composition and properties of biodiesel using principal component analysis (PCA) and artificial neural network (ANN). *Renewable Energy*, *168*, 632–646. https://doi.org/10.1016/j.renene.2020.12.078

Kingma, D. P., & Ba, J. (2017). *Adam: A Method for Stochastic Optimization* (arXiv:1412.6980). arXiv. https://doi.org/10.48550/arXiv.1412.6980

Kistelegdi, I., Horváth, K. R., Storcz, T., & Ercsey, Z. (2022). Building Geometry as a Variable in Energy, Comfort, and Environmental Design Optimization—A Review from the Perspective of Architects. *Buildings*, *12*(1), 69. https://doi.org/10.3390/buildings12010069

Liu, Y., Lee, T.-U., Rezaee Javan, A., Pietroni, N., & Xie, Y. M. (2024). Reducing the Number of Different Faces in Free-Form Surface Approximations Through Clustering and Optimization. *Computer-Aided Design*, *166*, 103633. https://doi.org/10.1016/j.cad.2023.103633

Mahdavinejad, M., Bazazzadeh, H., Mehrvarz, F., Berardi, U., Nasr, T., Pourbagher, S., & Hoseinzadeh, S. (2024). The impact of facade geometry on visual comfort and energy consumption in an office building in different climates. *Energy Reports*, *11*, 1–17. https://doi.org/10.1016/j.egyr.2023.11.021

McKay, M. D., Beckman, R. J., & Conover, W. J. (1979). Comparison of Three Methods for Selecting Values of Input Variables in the Analysis of Output from a Computer Code. *Technometrics*, *21*(2), 239–245. https://doi.org/10.1080/00401706.1979.10489755

Mehrotra, A., & Yi, H. (2023). Effect of adaptive intelligent sampling and machine-learning emulators in surrogate energy modeling of architectural massing. *Journal of Building Engineering*, *72*, 106614. https://doi.org/10.1016/j.jobe.2023.106614

Meng, X., & Karniadakis, G. E. (2020). A composite neural network that learns from multi-fidelity data: Application to function approximation and inverse PDE problems. *Journal of Computational Physics*, *401*, 109020. https://doi.org/10.1016/j.jcp.2019.109020

Pham, A.-D., Ngo, N.-T., Ha Truong, T. T., Huynh, N.-T., & Truong, N.-S. (2020). Predicting energy consumption in multiple buildings using machine learning for improving energy efficiency and sustainability. *Journal of Cleaner Production*, *260*, 121082. https://doi.org/10.1016/j.jclepro.2020.121082

Pottmann, H., Liu, Y., Wallner, J., Bobenko, A., & Wang, W. (2007). Geometry of Multi-layer Freeform Structures for Architecture. *ACM Transactions on Graphics*, *26*(3), 65. https://doi.org/10.1145/1275808.1276458

Queipo, N. V., Haftka, R. T., Shyy, W., Goel, T., Vaidyanathan, R., & Kevin Tucker, P. (2005). Surrogate-based analysis and optimization. *Progress in Aerospace Sciences*, *41*(1), 1–28. https://doi.org/10.1016/j.paerosci.2005.02.001

Sarker, I. H. (2021). Machine Learning: Algorithms, Real-World Applications and Research Directions. *SN Computer Science*, *2*(3), 160. https://doi.org/10.1007/s42979-021-00592-x

Senatore, G., & Piker, D. (2015). Interactive real-time physics. *Computer-Aided Design*, *61*, 32–41. https://doi.org/10.1016/j.cad.2014.02.007

Topuz, B., & Çakici Alp, N. (2023). Machine learning in architecture. *Automation in Construction*, *154*, 105012. https://doi.org/10.1016/j.autcon.2023.105012

Wang, B., Lu, W., & Zhang, Y. (2025). A graph-enabled parametric modeling approach for façade layout generative design. *Journal of Building Engineering*, *105*, 112481. https://doi.org/10.1016/j.jobe.2025.112481

Wang, H., Pellis, D., Rist, F., Pottmann, H., & Müller, C. (2019). Discrete geodesic parallel coordinates. *ACM Transactions on Graphics*, *38*(6), 1–13. https://doi.org/10.1145/3355089.3356541

Westermann, P., & Evins, R. (2019). Surrogate modelling for sustainable building design – A review. *Energy and Buildings*, *198*, 170–186. https://doi.org/10.1016/j.enbuild.2019.05.057

Yang, S., Lee, S., & Yee, K. (2023). Inverse design optimization framework via a two-step deep learning approach: Application to a wind turbine airfoil. *Engineering with Computers*, *39*(3), 2239–2255. https://doi.org/10.1007/s00366-022-01617-6